Rocking Damping of Arbitrarily Shaped Embedded Foundations

By Martha Fotopoulou,[1] Panos Kotsanopoulos,[2] George Gazetas,[3] and John L. Tassoulas[4]

Abstract: A simple analytical model is developed for estimating the rocking radiation damping coefficients of arbitrarily shaped rigid foundations embedded in an elastic homogeneous halfspace. The model, based on sound physical approximations that respect fundamental principles of dynamics and wave propagation, is calibrated with the help of rigorous numerical results from boundary element and finite element formulations. Results and comparisons are presented for a variety of basemat shapes (including the circle, rectangles with aspect ratio of up to ten, the strip, and T-shapes), for a wide range of embedment depths, and for complete, as well as partial, symmetric and nonsymmetric contact between the vertical side-walls and surrounding soil. Valuable insight is gained into the mechanics of radiation damping, and it is demonstrated quantitatively that, in practice, separation and slippage between side-walls and soil would appreciably affect damping for rocking only in the lateral direction (i.e., about the long axis of the basemat).

Introduction

This is the second of a two-paper sequence studying the rocking dynamic response $\theta = \theta_0 \exp(i\omega t)$ of rectangular and arbitrarily shaped foundations embedded in an elastic halfspace and subjected to harmonic excitation $M = M_0 \exp(i\omega t)$ of circular frequency ω (Fig. 1). The first paper (Hatzikonstantinou et al. 1989) presents results for estimating the static stiffnesses K_{rx} and K_{ry} and the dynamic stiffness coefficients, $k_{rx} = k_{rx}(\omega)$ and $k_{ry} = k_{ry}(\omega)$, of such foundations. The objective of this paper is to provide information for predicting the two radiation damping coefficients, $C_{rx} = C_{rx}(\omega)$ and $C_{ry} = C_{ry}(\omega)$, which represent the geometric spreading of energy by waves propagating away from the foundation. Recall that stiffness and damping terms combine as follows to give the dynamic moment-rotation ratio (impedance):

$$K_r k_r(\omega) + i\omega C_r(\omega) = \frac{M}{\theta} \quad \ldots\ldots (1)$$

in which $r = rx$ or ry depending on whether the rotation occurs about the longitudinal (x) or the lateral (y) axis, respectively. The moment M refers to the centroid of the foundation basemat. $C_{rx}(\omega)$ and $C_{ry}(\omega)$ can be interpreted as the "equivalent dashpot" coefficients in rocking.

Simple algebraic formulas are developed for predicting the two equivalent radiation dashpot coefficients. Such formulas, although calibrated with numerical data only for a homogeneous halfspace, may be readily extended to

[1]Student, Nat. Tech. Univ., Athens, Greece 10682.
[2]Student, Nat. Tech. Univ., Athens, Greece 10682.
[3]Prof. of Geotech. Engrg., Nat. Tech. Univ., Athens, Greece; present address: Dept. Civ. Engrg., State Univ. of New York, 212 Ketter Hall, Buffalo, N.Y. 14260.
[4]Assoc. Prof. of Civ. Engrg., Univ. of Texas, Austin, TX 78712.

Note. Discussion open until September 1, 1989. Separate discussions should be submitted for the individual papers in this symposium. To extend the closing date one month, a written request must be filed with the ASCE Manager of Journals. The manuscript for this paper was submitted for review and possible publication on February 19, 1988. This paper is part of the ***Journal of Geotechnical Engineering***, Vol. 115, No. 4, April, 1989. ©ASCE, ISSN 0733-9410/89/0004-0473/$1.00 + $.15 per page. Paper No. 23335.

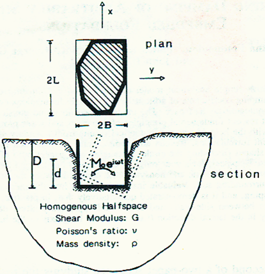

FIG. 1. Problem Geometry

encompass some more realistic soil profiles.

In reality, in addition to loss due to radiation, energy is also dissipated by hysteretic action in the soil, conveniently expressed through a frequency-independent material damping ratio, β. The combined radiation-hysteretic dashpot coefficients $C_r(\omega, \beta)$ can be approximated (Lysmer 1980) as

$$C_r(\omega, \beta) \approx C_r(\omega) + \frac{2K_r k_r(\omega)}{\omega}\beta \quad \text{(2)}$$

This approximation is very reasonable for the homogeneous halfspace studied herein, but it is not generally true for layered deposits with sharp velocity contrasts.

It is worth mentioning that the dynamic rocking of embedded foundations has received significant attention in the past [see Berredugo and Novak (1982), Day (1977), Dominquez and Roesset (1978), Kausel and Ushijima (1979), Kausel and Roesset (1975), Roesset (1980), Tassoulas (1986), and Wolf (1985)]. In fact, since a rocking surface foundation usually generates very small amounts of radiation damping and may thus experience high amplitudes if at resonance, embedment is one of the best ways to alleviate such a problem by significantly increasing the generated damping.

Development of Method for Embedded Rectangular Foundation

Fig. 2 shows the available numerical results for damping of embedded foundations. Most of these results were obtained by the writers using a boundary-element formulation (Hatzikonstantinou et al. 1989); also included, however, are all the available results in the known literature. It is

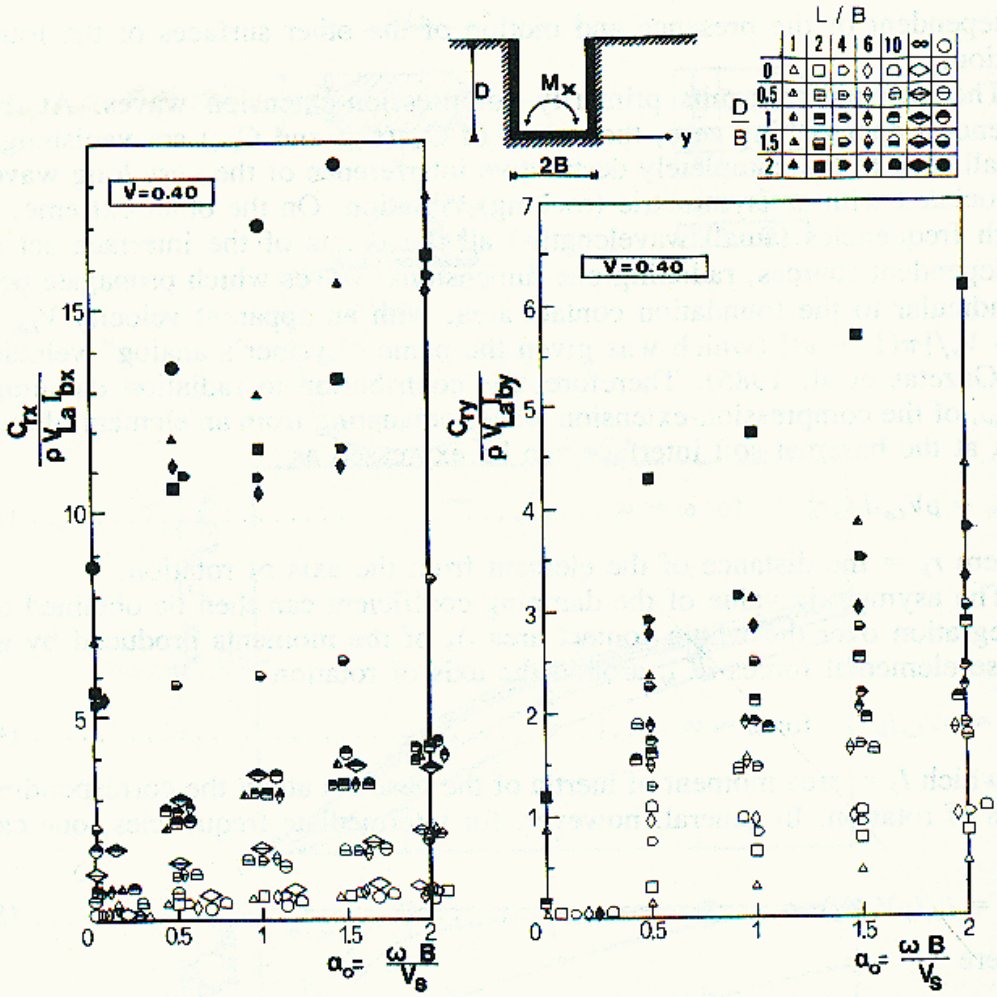

FIG. 2. Fully Embedded Rectangular Foundations: Effect of Depth and Aspect Ratios on Rocking Radiation Dashpot Coefficients [Data for Rectangles from this Study, for Strip from Wolf (1985), and for Circle from Day (1977)]

evident that both the depth of embedment and the shape of the basemat may have a very significant effect on radiation damping. Thus there is a need to develop a method for readily (and reliably) estimating damping in practice. The proposed method is first explained for a rectangular prismatic foundation that has a uniform-along-the-perimeter height d of sidewall-soil contact.

Simple Physical Model

The value of the two radiation-damping coefficients reflects the vibrational energy transmitted into the soil and carried away by outward and downward spreading waves, which are generated at every point on the soil-foundation interface. In general, the damping coefficients increase with increasing area of contact. During rocking of embedded foundations, in addition to compression-extension waves originating at the basemat, shearing and compression-extension waves are emitted from the vertical sidewall surfaces, depending on whether a particular side is parallel, perpendicular, or inclined to the direction of the rocking moment. A key assumption of the proposed model is that the amount of damping contributed by the motion of each surface is

independent of the presence and motion of the other surfaces of the foundation.

The basemat transmits primarily compression-extension waves. At frequencies approaching zero, the values of C_{br} (C_{brx} and C_{bry}) are vanishingly small, due to the completely destructive interference of the very long waves associated with antisymmetric (rocking) vibration. On the other extreme, at high frequencies (small wavelengths) all the points of the interface act as independent sources, radiating one-dimensional waves which propagate perpendicular to the foundation contact area, with an apparent velocity $V_{La} \approx 3.4\ V_s/[\pi(1-\nu)]$ (which was given the name "Lysmer's analog" velocity in Gazetas et al. 1985). Therefore, the contribution to radiation damping, dC_{br}, of the compression-extension waves emanating from an element of area dA_b at the basemat-soil interface can be expressed as

$$dC_{br} \approx \rho V_{La}\, dA_b r_b^2 \qquad \text{for } \omega \approx \infty \quad \ldots\ldots (3)$$

where r_b = the distance of the element from the axis of rotation.

The asymptotic value of the damping coefficient can then be obtained by integration over the whole contact area A_b of the moments produced by all these elemental forces dC_{br} around the axis of rotation

$$C_{br} \approx \rho V_{La} I_b \qquad \text{for } \omega \approx \infty \quad \ldots\ldots (4)$$

in which I_b = area moment of inertia of the basemat about the corresponding axis of rotation. In general, however, for intermediate frequencies, one can set

$$C_{br} = \tilde{c}_{or}(\rho V_{La} I_b) \quad \ldots\ldots (5)$$

where

$$\tilde{c}_{0r} = \tilde{c}_{0r}\left(a_0; \frac{L}{B}\right) \quad \ldots\ldots (6)$$

The dimensionless coefficients $\tilde{c}_{0r}$ ($\tilde{c}_{0rx}$ and $\tilde{c}_{0ry}$) are assumed to be identical for surface, trench, and embedded foundations, and can be obtained from Fig. 3.

The sidewalls that are perpendicular to the direction of the imposed motion (or, in other words, parallel to the vector of the imposed rocking moment) perform two motions (Fig. 1):

1. A rotation $\theta(t)$ around the base axis x or y, depending on the mode, equal to the imposed angle of rotation of the (rigid) foundation. Owing to this motion the wall emits compression-extension waves that are assumed to propagate with an apparent velocity equal to V_{La}. It is further assumed that the fact the sidewalls are vertical rather than horizontal surfaces does not influence the asymptotic value of radiation damping and thus Eq. 4 is still applicable. Therefore, the contribution to radiation damping C_{wr} of a rocking sidewall can be expressed as

$$C_{wr1} = \tilde{c}_1(\rho V_{La} I_{wr}) \quad \ldots\ldots (7)$$

in which the dimensionless coefficient $\tilde{c}_1$ is

$$\tilde{c}_1 = \tilde{c}_1\left(a_0; \frac{d}{D}, \frac{D}{B}, \frac{L}{B}, \nu\right) \quad \ldots\ldots (8)$$

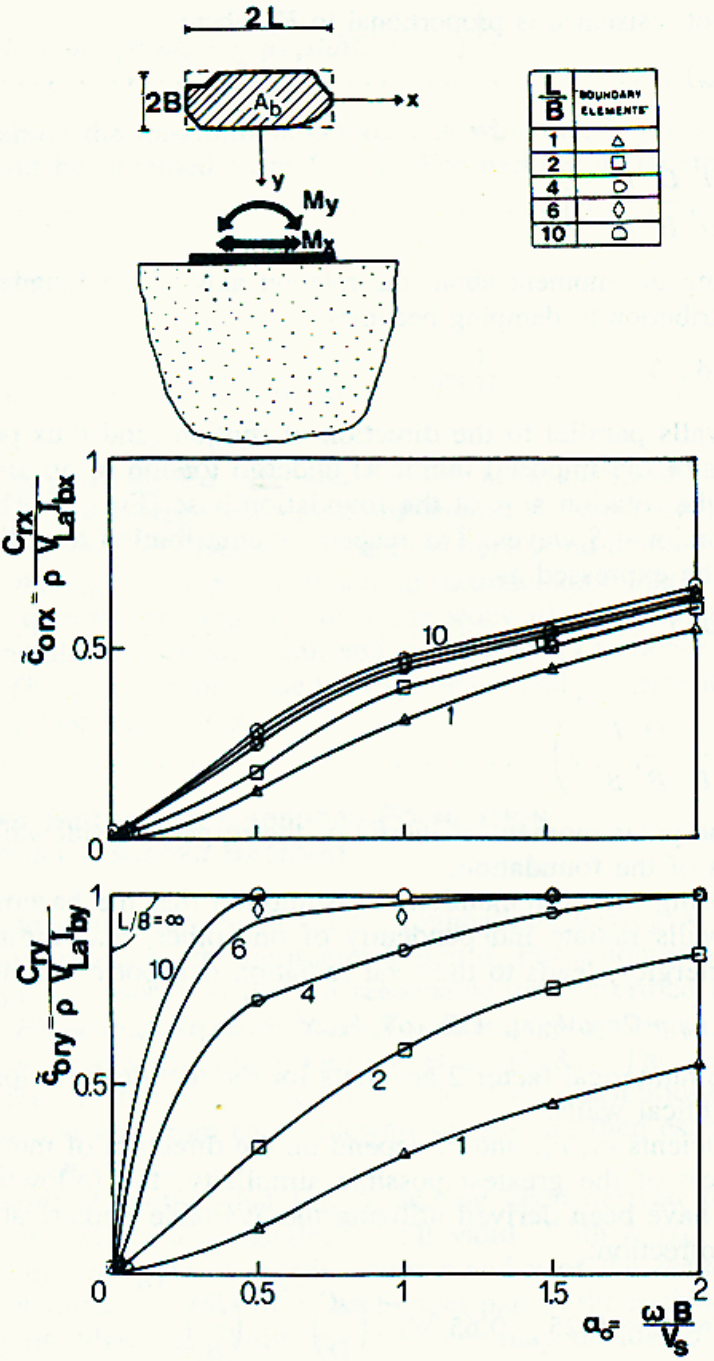

FIG. 3. Charts for Rocking Radiation Dashpot Coefficients of Surface Foundations

and I_{wr} = the sidewall area moment of inertia about the projection of the axis of rotation (x or y) onto the plane of the particular sidewall.

2. A vertical vibration with amplitude equal to the product $\theta(t) \cdot \Delta$, in which Δ = the distance of the particular sidewall from the foundation rotation axis (x or y). For rectangular shapes, $\Delta = B$ when the rotation takes place around the longitudinal axis x, and $\Delta = L$ when around the lateral axis y. Due to this motion, the sidewall emits shearing waves propagating with velocity V_s. The re-

sultant dashpot resistance is proportional to F, where

$$F = \tilde{c}_2(\rho V_s A_{wr}) \quad (9)$$

and

$$\tilde{c}_2 = \tilde{c}_2\left(a_0; \frac{d}{D}, \frac{D}{B}, \frac{L}{B}, \nu\right) \quad (10)$$

By considering the moment about the rotation axis of the foundation, the respective contribution to damping becomes

$$C_{wr_2} = \tilde{c}_2 \rho V_s A_{wr} \Delta^2 \quad (11)$$

The sidewalls parallel to the direction of motion (and thus perpendicular to the vector of the imposed moment) undergo torsion of an angle equal to $\theta(t)$ around the rotation axis of the foundation base (Fig. 1). The generated waves are torsional S waves. The respective contribution to radiation damping C_{wt} can be expressed as

$$C_{wt} = \tilde{c}_3(\rho V_s J_{wt}) \quad (12)$$

with

$$\tilde{c}_3 = \tilde{c}_3\left(a_0; \frac{d}{D}, \frac{D}{B}, \frac{L}{B}, \nu\right) \quad (13)$$

and J_{wt} = the polar moment of inertia of the respective sidewall around the rotation axis of the foundation.

Finally, using the aforementioned assumption that the basemat and each of the sidewalls radiate independently of one other, and summing up the respective energies, leads to the total radiation dashpot coefficient:

$$C_r = c_{0r}\rho V_{La} I_{bi} + 2c_1 \rho V_{La} I_{wr} + 2c_2 \rho V_s A_{wr} \Delta^2 + 2c_3 \rho V_s J_{wt} \quad (14)$$

in which the numerical factor 2 accounts for the identical motion of the two opposite identical walls.

The coefficients c_1, c_2, and c_3 depend on the direction of motion (x or y). In the interest of the greatest possible simplicity, the following algebraic expressions have been derived utilizing the available numerical data:

for the x-direction:

$$\tilde{c}_1 = \tilde{c}_2 = \tilde{c}_3 \equiv \tilde{c}_{rx} \approx 0.25 + 0.65\sqrt{a_0}\left(\frac{d}{D}\right)^{-a_0/2}\left(\frac{D}{B}\right)^{-1/4} \quad (15a)$$

for the y-direction:

$$\tilde{c}_1 = \tilde{c}_2 = \tilde{c}_3 \equiv \tilde{c}_{ry} \approx 0.25 + 0.65\sqrt{a_0}\left(\frac{d}{D}\right)^{-a_0/2}\left(\frac{D}{L}\right)^{-1/4} \quad (15b)$$

Eqs. 14–15 provide the radiation dashpot coefficients, C_{rx} and C_{ry}, for a rectangular foundation $2L$ by $2B$ placed at depth D below the ground surface, and having vertical sidewalls of uniform-along-the-perimeter height d. Eq. 14 can be written more explicitly as follows:

$$C_{rx} = \frac{4}{3}\rho V_{La} B^3 L \tilde{c}_{0rx}$$

$$+ \left[\frac{4}{3}\rho V_{La} d^3 L + 4\rho V_s B^2 dL + \frac{4}{3}\rho V_s B d(B^2 + d^2)\right]\tilde{c}_{rx} \quad \ldots\ldots\ldots\ldots\ldots\ldots \quad (16a)$$

for rocking about the longitudinal (x) axis, in which $\tilde{c}_{rx}$ is given by Eq. 15*a* and $\tilde{c}_{0rx}$ should be obtained from Fig. 3. For rocking about the lateral (y) axis

$$C_{ry} = \frac{4}{3}\rho V_{La} B^3 L \tilde{c}_{0ry}$$

$$+ \left[\frac{4}{3}\rho V_{La} d^3 B + 4\rho V_s L^2 dB + \frac{4}{3}\rho V_s L d(L^2 + d^2)\right]\tilde{c}_{ry} \quad \ldots\ldots\ldots\ldots\ldots\ldots \quad (16b)$$

in which $\tilde{c}_{ry}$ is given by Eq. 15*b* and $\tilde{c}_{0ry}$ should be obtained from Fig. 3.

Note that d in the preceding equations should be interpreted as the "effective" sidewall height, over which there is very good contact between the sidewall and the surrounding soil. It should be understood that d can be equal to or smaller than the nominal height of the sidewall, depending on whether separation and sliding between wall and soil are likely to occur near the top of the wall. The engineer may use his experience and judgement in deciding on the appropriate value of d.

Extension of Method to Embedded Foundation with Arbitrarily Shaped Basemat

This section also refers to prismatic foundations having a sidewall-soil contact of uniform-along-the-perimeter height d. For a nonrectangular basemat, the engineer must first draw a reasonable circumscribed rectangle $2B$ by $2L$ ($L > B$), using common sense. For examples see Figs. 1, 3, 9, and 12, as well as several figures in Gazetas et al. (1985). The results are *not* sensitive to the exact circumscribed rectangle. The contributions to damping from the basemat and from each sidewall surface are then estimated as described in the following.

For the basemat, notice that Eq. 5, having been derived for a general shape and not just for a rectangle, is still valid. With I_b (I_{bx} and I_{by}), we denote the area moments of inertia about x and y of the *actual* soil-foundation contact surface. If loss of contact under part of the rocking foundation (e.g., along its edges) is likely, the engineer may decide to discount the contribution of that part when computing I_b.

The contribution of the vertical sidewall is computed with the help of the circumscribed rectangular prism of dimensions $2B$ by $2L$ by d. A very simple approximate relationship is found between the damping C_{rect} generated by this fictitious circumscribed rectangular prism and the damping C_{actual} produced by the actual sidewall surface. Their ratio is roughly equal to the ratio of the area moments of inertia of the circumscribed rectangular base and the actual basemat. Thus, to derive C_{actual}, we simply multiply C_{rect} by the ratio $I_{bx}/(4LB^3/3)$ or by $I_{by}/(4BL^3/3)$, for rocking about x or y, respectively. Noting that C_{rect} is given by the last three terms on the right-hand side of Eqs. 16 leads to the following simple expressions for the total radiation dashpot coefficients of the arbitrarily shaped foundation:

$$C_{rx} \approx \rho V_{La} I_{bx} \tilde{c}_{0rx} + \left[\rho V_{La} I_{bx} \frac{d^3}{B^3} + 3\rho V_s I_{bx} \frac{d}{B} + \rho V_s I_{bx} \frac{d}{L} \left(1 + \frac{d^2}{B^2} \right) \right] \tilde{c}_{rx} \ldots \quad (17a)$$

$$C_{rx} \approx \rho V_{La} I_{bx} \tilde{c}_{0rx} + \left[\rho V_{La} I_{bx} \frac{d^3}{B^3} + 3\rho V_s I_{bx} \frac{d}{B} + \rho V_s I_{bx} \frac{d}{L} \left(1 + \frac{d^2}{B^2} \right) \right] \tilde{c}_{rx} \ldots \quad (17a)$$

in which the dimensionless $\tilde{c}$ coefficients are obtained for the circumscribed rectangle (Eq. 15).

Comparison with Numerical Data for Fully Embedded Foundations

This section evaluates the developed simple method with foundations embedded at depth D and having sidewalls of height $d = D$ in perfect contact with the surrounding soil. The combined effect of the depth ratio D/B and the aspect ratio L/B on the normalized damping coefficients $C_{rx}/\rho V_{La} I_{bx}$ and $C_{ry}/\rho V_{La} I_{by}$ of rectangular foundations has already been shown in Fig. 2. It is evident that while increasing D/B would invariably increase radiation damping, the magnitude of the increase is a function of both L/B and the direction of oscillation.

A summary of a comprehensive comparison between the predictions of the developed simple method (Eqs. 16 and 17) and rigorous numerical results is shown as follows: in Figs. 4, 5, and 6 for rectangles with $L/B = 1$, 4,

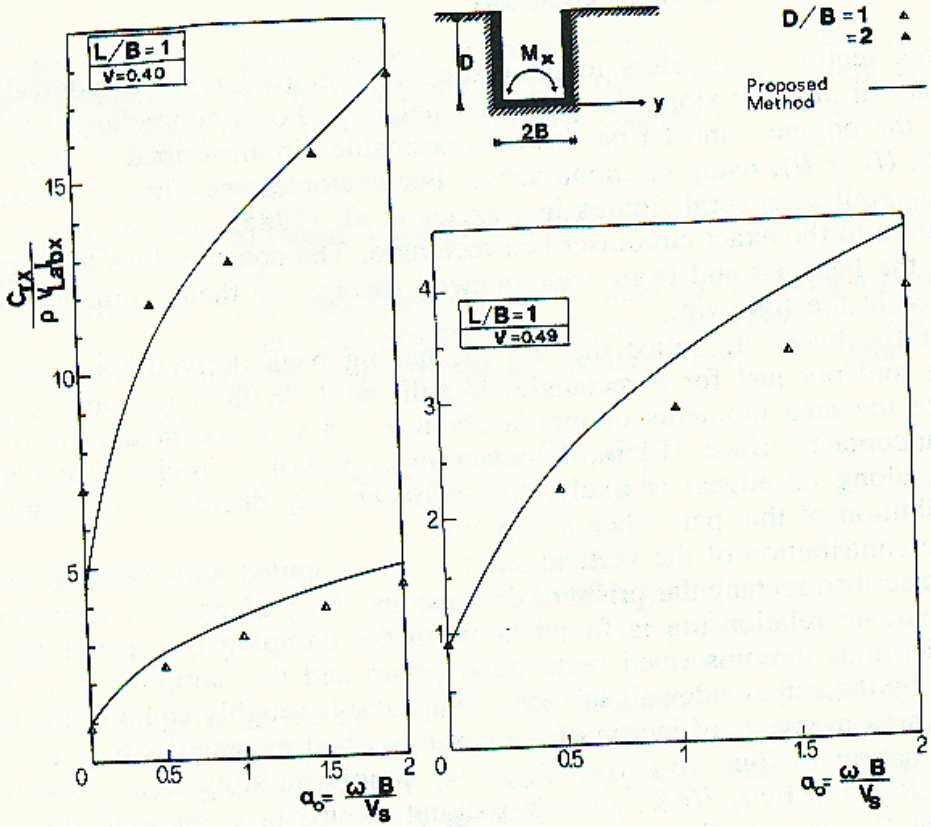

FIG. 4. Comparison of Proposed-Method Predictions with Boundary-Element Results for Damping of Square Embedded Foundations for $\nu = 0.40$ and $\nu = 0.49$

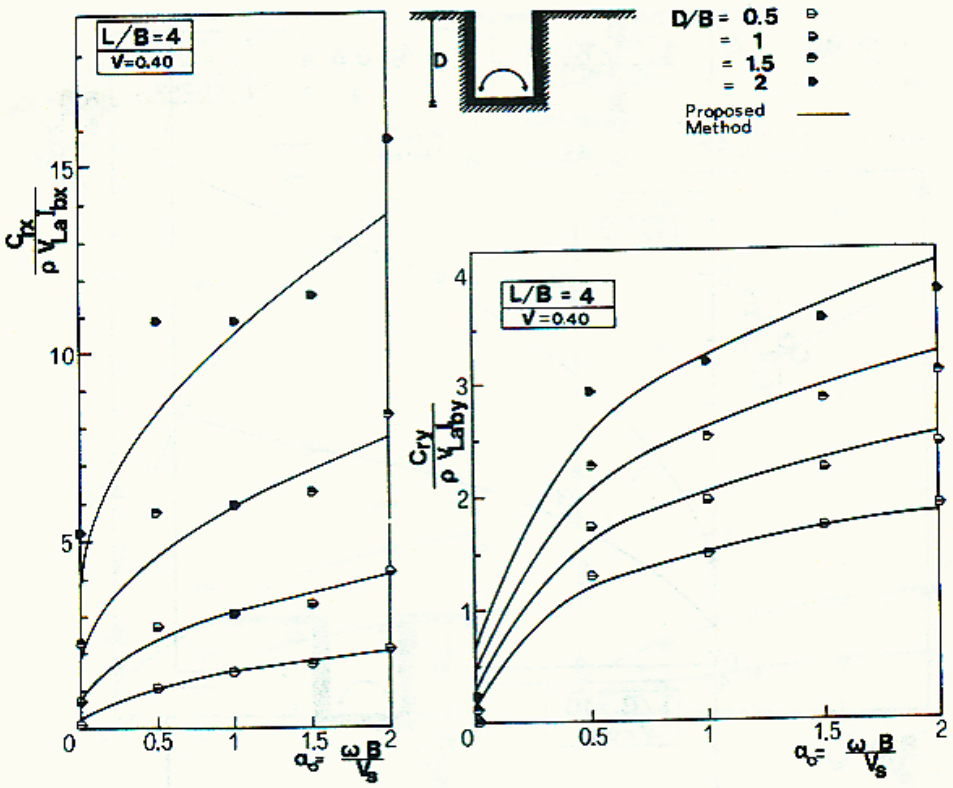

FIG. 5. Comparison of Proposed-Method Predictions with Boundary-Element Results for Damping of Rectangular (L/B = 4) Embedded Foundations Rocking about x (Left) or y (Right) Axis

and 10; in Fig. 7 for strip and circle; and in Figs. 8 and 9, for T-shapes. The solid lines in these figures plot Eq. 16 or Eq. 17. The numerical data points are from the boundary element solution, except those for the cylindrical foundation [from Day (1977)] and those for the strip [from Wolf (1985)]. Notice again the substantial increase of radiation damping with embedment.

The performance of the developed simple radiation damping method is very good in all cases studied (not only those shown in Figs. 4–9), for all frequencies up to $a_0 = 2$, and three values of Poisson's ratio: $\nu = 0.33$, 0.40, and 0.49. The maximum error in the considered range of parameters does not exceed 25% and in most cases remains below a mere 5%. Particularly encouraging is the excellent accord between the developed simple model and the rigorous solution for the two T-shaped deeply embedded foundations.

Comparison with Numerical Data for Partially Embedded Foundations

This section studies foundations embedded at depth D but having sidewalls that are in contact with the surrounding soil only over a height d, less than D.

The effect of the ratio of the sidewall-soil contact height to the trench depth, d/D, is shown in Figs. 10 and 11. Plotted are the ratios $C_{rx}/\rho V_{La} I_{bx}$

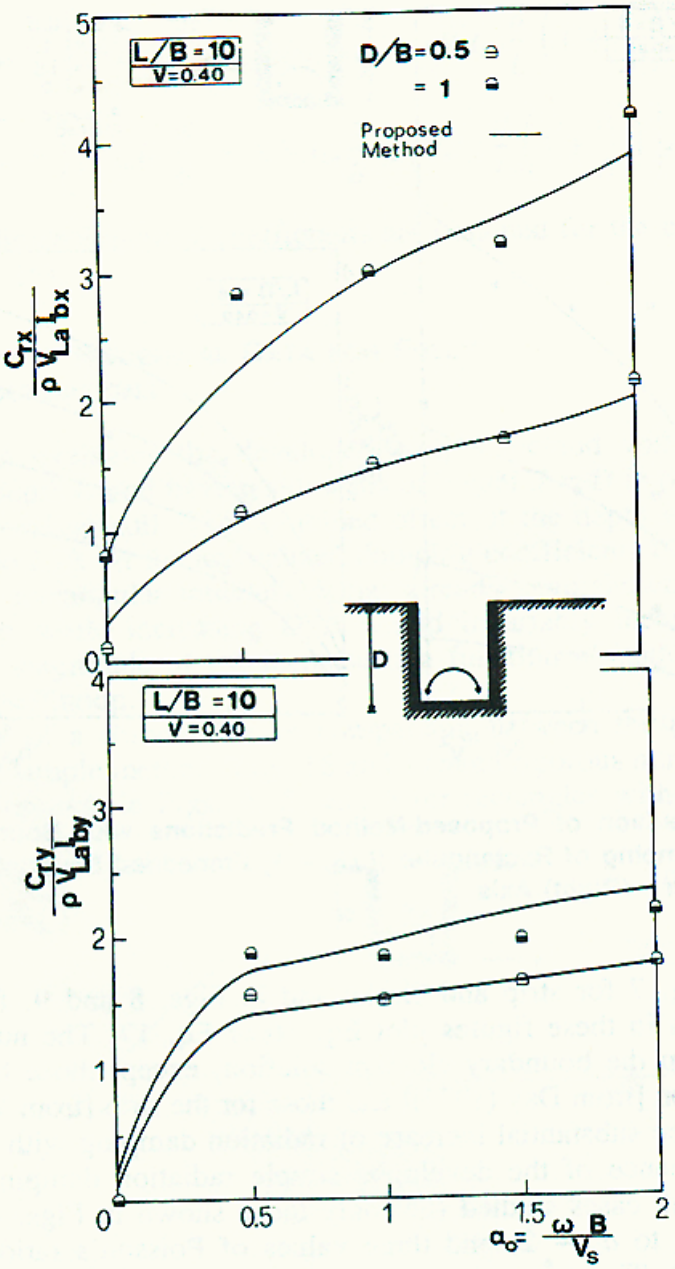

FIG. 6. Comparison of Proposed-Method Predictions with Boundary-Element Results for Damping of Rectangular (L/B = 10) Embedded Foundations Rocking about x (Top) or y (Bottom) Axis

and $C_{ry}/\rho V_{La} I_{by}$ versus a_0 and d/D, for foundations with aspect ratios L/B = 4 and 10 and a trench depth $D = B$. Three or four values of d/D are considered, ranging from zero (foundation in an open trench without sidewalls) to one (fully embedded foundation).

A consistent noteworthy trend is evident in these figures. C_{rx}, for rotation around the longitudinal x-axis, is quite sensitive to variations in d/D. For instance, when d/D decreases from 1 (full embedment) to 2/3, C_{rx} falls to about 70% of its fully embedded value. This separation and slippage that may occur between the walls and the backfill near the ground surface will

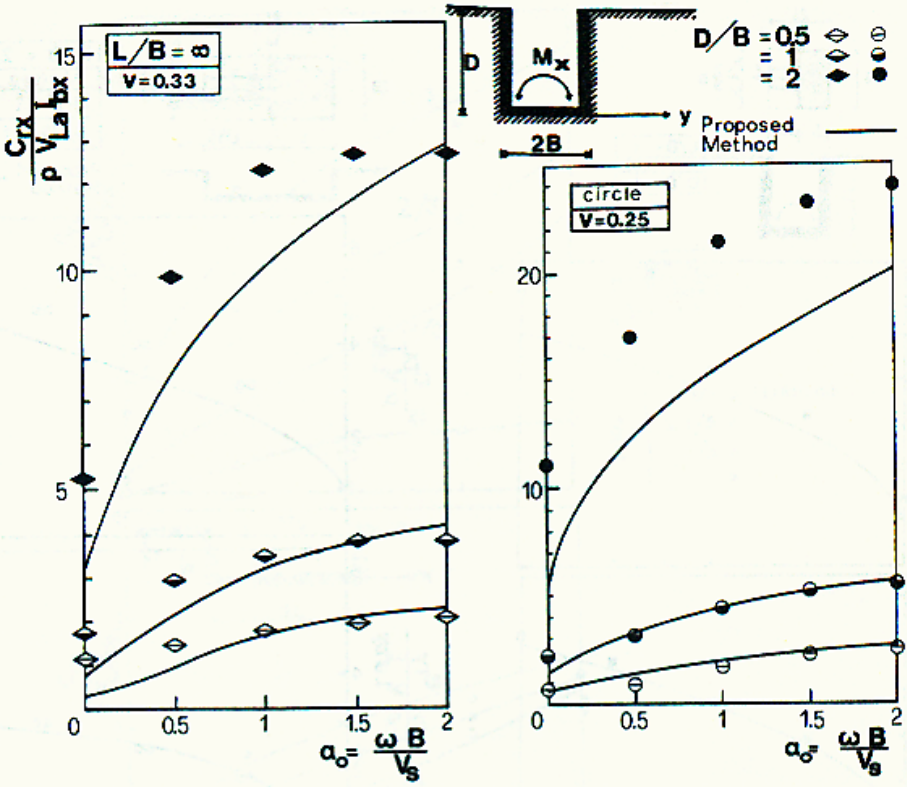

FIG. 7. Comparison of Proposed-Method Predictions with Numerical Results for Damping of Strip (Wolf 1985) and Circular (Day 1977) Embedded Foundations

probably have a large effect on radiation damping in rocking around the x-axis.

On the other hand, the variation of d/D has a negligible effect on the damping coefficient C_{ry} for rocking around the y-axis; the engineer need not worry a great deal about separation/slippage near the ground surface.

This behavior, which the developed simple method predicts reasonably well, can be physically explained as follows: When the foundation is oscillating in rocking about the longitudinal axis x, the surfaces mainly contributing to damping are the upper and lower parts of the sidewalls that are parallel to that axis (perpendicular to the motion). This is because of their relatively large size (length $2L > 2B$) and the fact that they emit compression-extension, rather than shear, waves. Thus, a small slippage at the contact surface between soil-walls near the ground surface will reduce the moment arm of these major normal tractions and will thereby considerably reduce the damping coefficient, C_{rx}. Whereas, when the foundation is subjected to rotation about the lateral axis y, the largest sidewall surfaces are perpendicular to that axis and emit torsional shear rather than compression waves. Thus, the largest contribution to radiation damping arises from the couples of opposite vertical shear tractions distributed near the two edges of each long sidewall, with a moment arm essentially $2L$. The moment arm of such traction is hardly influenced by changes in the height of the sidewall d, thus the insensitivity of C_{ry} to d/D.

The overall performance of the presented simple model is very good in all cases studied.

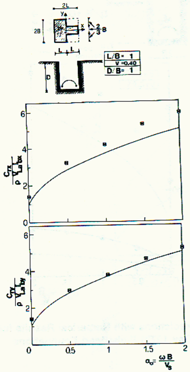

FIG. 8. Comparison of Proposed-Method Predictions with Boundary-Element Results for Damping of T-Shaped Embedded Foundations (L/B = 1, ν = 0.40) Rocking about x (Top) or y (Bottom) Axis

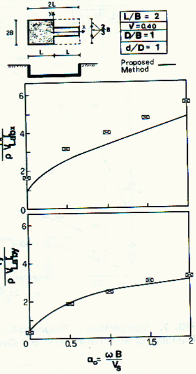

FIG. 9. Comparison of Proposed-Method Predictions with Boundary-Element Results for Damping of T-Shaped Embedded Foundations (L/B = 2, ν = 0.40) Rocking about x (Top) or y (Bottom) Axis

Generalization of Method

The aforementioned method refers to foundations with uniform sidewall height and solid sidewalls along the perimeter. However, it can be extended to foundations with nonuniform and nonsymmetric wall height. The developed expressions can be generalized so that the contribution of every part of the sidewall is isolated from the whole radiation damping of foundation. Thus, for example, the case of two opposite sidewalls performing the same motion but having a different height d and a different type of contact with the surrounding soil can be handled with this method. The expressions that represent the generalization of method are

$$C_{rx} = \rho V_{La} I_{bx} \bar{c}_{0rx} + \frac{\rho V_{La} I_{bx}}{2B^3}\sum_{i=1}^{n}(\bar{c}_{ri}\alpha_i d_{ri}^3) + \frac{3\rho V_s I_{bx}}{2B}\sum_{i=1}^{n}(\bar{c}_{ri}\epsilon_i d_{ri})$$

$$+ \frac{\rho V_s I_{bx}}{2L}\sum_{i=1}^{m}\left\{\bar{c}_{ti}\delta_i d_{ti}\left[1+\left(\frac{d_{ti}}{B}\right)^2\right]\right\} \quad \text{(18a)}$$

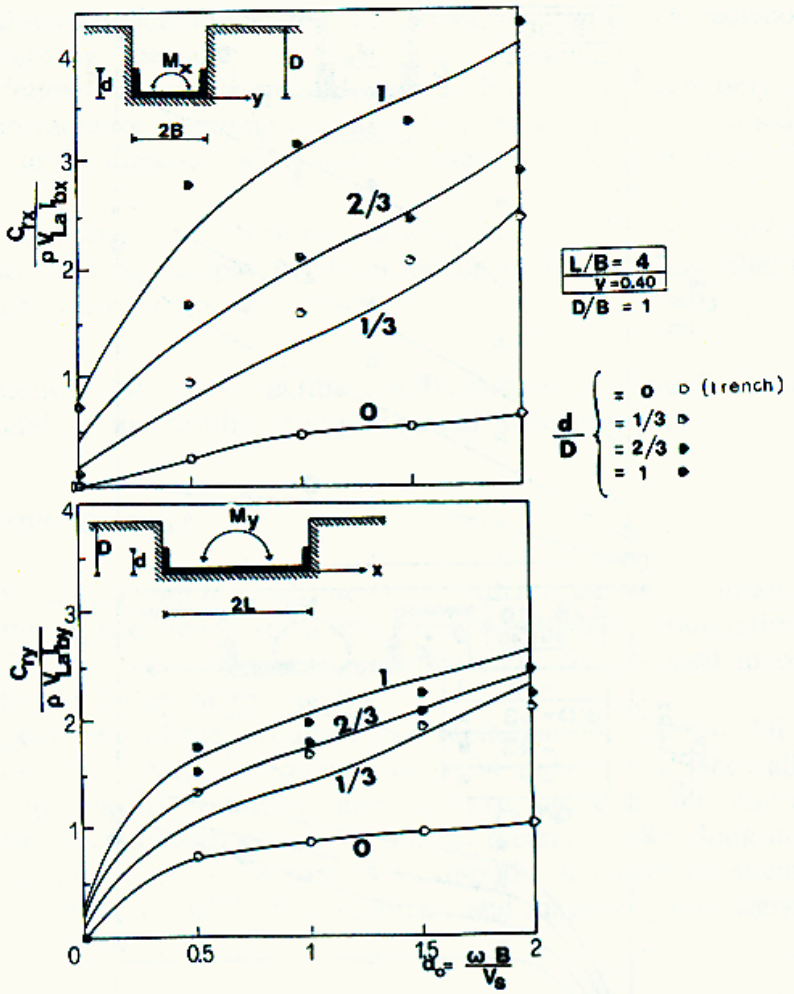

FIG. 10. Comparison of Proposed-Method Predictions with Boundary-Element Results for Partially Embedded Rectangular ($L/B = 4$) Foundations ($d/D = 0$, 1/3, 2/3, and 1) Rocking about x (Top) or y (Bottom)

$$C_{ry} = \rho V_{La} I_{by} \tilde{c}_{0ry} + \frac{\rho V_{La} I_{by}}{2L^3} \sum_{i=1}^{n} (\tilde{c}_{ri} \alpha_i d_{ri}^3) + \frac{3\rho V_s I_{by}}{2L} \sum_{i=1}^{n} (\tilde{c}_{ri} \epsilon_i d_{ri})$$

$$+ \frac{\rho V_s I_{by}}{2B} \sum_{i=1}^{m} \left\{ \tilde{c}_{ti} \delta_i d_{ti} \left[1 + \left(\frac{d_{ti}}{L} \right)^2 \right] \right\} \quad \ldots\ldots\ldots\ldots\ldots\ldots\ldots\ldots\ldots\ldots\ldots\ldots \quad (18b)$$

where

$$\tilde{c}_{ri} = 0.25 + 0.65 \sqrt{a_0} \left(\frac{d_{ri}}{D} \right)^{-(a_0/2)} \left(\frac{D}{B} \right)^{-1/4} \quad \ldots\ldots\ldots\ldots\ldots\ldots\ldots\ldots\ldots\ldots\ldots\ldots \quad (19a)$$

$$\tilde{c}_{ti} = 0.25 + 0.65 \sqrt{a_0} \left(\frac{d_{ti}}{D} \right)^{-(a_0/2)} \left(\frac{D}{B} \right)^{-1/4} \quad \ldots\ldots\ldots\ldots\ldots\ldots\ldots\ldots\ldots\ldots\ldots\ldots \quad (19b)$$

in Eq. 18*a* and

$$\tilde{c}_{ri} = 0.25 + 0.65 \sqrt{a_0} \left(\frac{d_{ri}}{D} \right)^{-(a_0/2)} \left(\frac{D}{L} \right)^{-1/4} \quad \ldots\ldots\ldots\ldots\ldots\ldots\ldots\ldots\ldots\ldots\ldots\ldots \quad (20c)$$

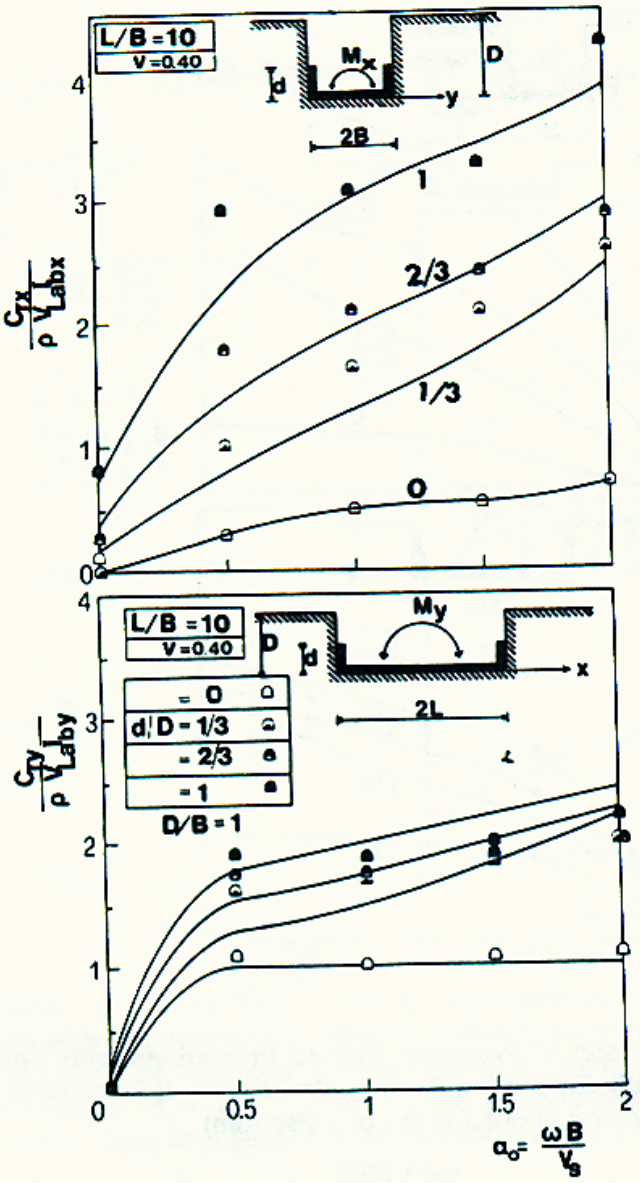

FIG. 11. Comparison of Proposed-Method Predictions with Boundary-Element Results for Partially Embedded Rectangular (L/B = 10) Foundations (d/D = 0, 1/3, 2/3, and 1) Rocking about x (Top) or y (Bottom) Axis

$$\tilde{c}_{ti} = 0.25 + 0.65\sqrt{a_0}\left(\frac{d_{ti}}{D}\right)^{-(a_0/2)}\left(\frac{D}{L}\right)^{-1/4} \quad \ldots\ldots\ldots\ldots\ldots\ldots\ldots\ldots\ldots\ldots \quad (20b)$$

in Eq. 18*b*. In these expressions:

1. n = the number of segments in which we divide the projection of sidewalls onto a plane parallel to the rocking axis. The division is done so that every segment has a constant height d_{ri}.
2. m = the number of segments in which we divide the projection of sidewalls onto a plane perpendicular to the rocking axis. The division is done so that every segment has a constant height d_{ti}.
3. α_i = numerical coefficient expressing empirically the quality of contact at

the sidewall-backfill interface. It refers only to the contribution to radiation damping C_{wr_1} of a rocking sidewall.

4. ϵ_i = numerical coefficient similar to a_i (Eq. 14). It refers only to the contribution to radiation damping c_{wr_2} from the vertical motion of a sidewall perpendicular to the direction of the imposed motion. It is equal to zero for smooth sidewalls.

5. δ_i = numerical coefficient similar to a_i (Eq. 14). It refers only to the contribution to radiation damping c_{wt} from torsion of a sidewall parallel to motion. It is equal to zero for smooth sidewalls.

The engineer may estimate the coefficients α_i, ϵ_i, and δ_i, based on experience and on the results of experimental measurements.

Illustrative Example

The foregoing formulas and charts are utilized herein to obtain estimates of the damping coefficient for a hypothetical embedded foundation sketched in Fig. 12. The chosen basemat is deliberately complicated in order to illustrate the flexibility of the method.

The aspect ratio of the circumscribed rectangle is $L/B = 4$. Of interest is the C_{rx} for an excitation frequency $\omega = 34$ rad/s. The sidewall height d equal to eight meters is uniform along part of the perimeter. Along the part ab, the effective sidewall height is only six meters, while along ac, no sidewall exists. The wall in the part ab is smooth, and thus no shear tractions can arise from the backfill. The geometry and material parameters are given in Fig. 12, from which

$$a_0 = \frac{\omega B}{V_s} = \frac{34 \times 7.5}{170} = 1.5 \quad \ldots\ldots\ldots\ldots\ldots\ldots\ldots\ldots\ldots\ldots\ldots\ldots\ldots\ldots\ldots\ldots\ldots\ldots \quad (21)$$

The damping coefficient C_{rx} is computed with the help of Eq. 18.

From Fig. 3, for $a_0 = 1.5$ and $L/B = 4$ we have $c_0 = 0.518$. For rocking about the x-axis, $\bar{c}_{0rx} = 0.52$, $\nu = 0.40$, $B = 7.50$ m, $L = 30$ m, $D = 8$ m, $d_{r_1} = 8$ m (projection be), $a_1 = 1$, $\epsilon_1 = 1$, $d_{r_2} = 8$ m (projection cd), $\alpha_2 = 0.75$, $\epsilon_2 = 0.75$, $n = 2$, $d_{t_1} = 8$ m (projection ed), $\delta_1 = 1$, $d_{t_2} = 6$ m (projection ab), $\delta_2 = 0$ (smooth sidewall), and $n = 2$. Thus

$$\bar{c}_{r1} = 0.25 + 0.65 \times \left[1.50 \times \left(\frac{8}{8}\right)^{-1.5} \times \left(\frac{8}{7.50}\right)^{0.5}\right]^{0.5} = 1.03 \quad \ldots\ldots\ldots \quad (22a)$$

$$\bar{c}_{r2} = 0.25 + 0.65 \times \left[1.50 \times \left(\frac{8}{8}\right)^{-1.5} \times \left(\frac{8}{7.50}\right)^{0.5}\right]^{0.5} = 1.03 \quad \ldots\ldots\ldots \quad (22b)$$

$$\bar{c}_{t1} = 0.25 + 0.65 \times \left[1.50 \times \left(\frac{8}{8}\right)^{-1.5} \times \left(\frac{8}{7.50}\right)^{0.5}\right]^{0.5} = 1.03 \quad \ldots\ldots\ldots \quad (22c)$$

$$\bar{c}_{t2} = 0.25 + 0.65 \times \left[1.50 \times \left(\frac{6}{8}\right)^{-1.5} \times \left(\frac{8}{7.50}\right)^{0.5}\right]^{0.5} = 1.22 \quad \ldots\ldots\ldots \quad (22d)$$

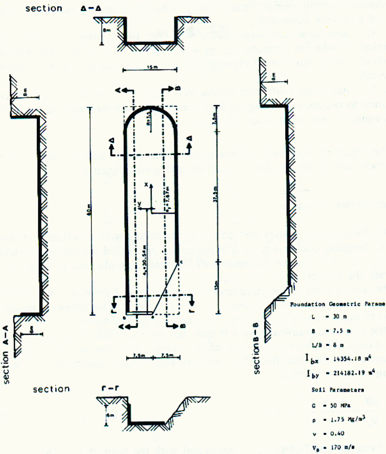

FIG. 12. Illustrative Example: Geometry and Material Parameters

with

$$\rho V_{La} I_{bx} = 7.7 \times 10^6 \text{ kN}\cdot\text{m}\cdot\text{s} \quad (23a)$$

and

$$\rho V_s I_{bx} = 4.27 \times 10^6 \text{ kN}\cdot\text{m}\cdot\text{s} \quad (23b)$$

Eq. 18 leads to

$$C_{rx} = 7.7 \times 10^6 \times 0.52 + \frac{7.7 \times 10^6}{2 \times 7.5^3} \times [1.03 \times 8^3 + 1.03 \times 0.75 \times 8^3]$$

$$+ \frac{3 \times 4.27 \times 10^6}{2 \times 7.5} \times [1.03 \times 8 + 1.03 \times 0.75 \times 8] + \frac{4.27 \times 10^6}{2 \times 30}$$

$$\times \{1.03 \times 8 \times \left[1 + \left(\frac{8}{7.5}\right)^2\right] + 1.22 \times 0 \times 6$$

$$\times \left[1 + \left(\frac{6}{7.5}\right)^2\right]\Bigg\} = 4.00 \times 10^6 + 8.42 \times 10^6 + 12.31$$

$$\times 10^6 + 1.25 \times 10^6 = 26 \times 10^6 \text{ kN} \cdot \text{m} \cdot \text{s} \quad \text{..... (24)}$$

Conclusions

The main conclusions of this paper are:

1. The developed simple analytical method for radiation damping of rocking embedded foundations is in very good agreement with far more sophisticated rigorous numerical formulations. The model can predict with remarkable consistency even detailed trends observed in the numerical results.
2. Separation and slippage that may occur between the walls and the backfill near the ground surface will probably have a large effect on radiation damping in rocking around the longitudinal axis. On the other hand, the engineer does not have much to worry about such separation/slippage in rocking about the lateral y-axis (i.e., for motion in the longitudinal direction).
3. The developed method is versatile in that it can handle arbitrarily shaped basemats as well as partial, symmetric and nonsymmetric, types of sidewall-soil contact. Extension of the method to apply to inhomogeneous profiles is also possible, although not addressed herein.

Appendix I. References

Berredugo, Y. O., and Novak, M. (1982). "Coupled horizontal and rocking vibrations of embedded footings." *Can. Geotech. J.*, 9(2), 477–497.

Day, S. M. (1977). "Finite element analysis of seismic scattering problems." thesis presented to the University of California at San Diego, La Jolla, Calif., in partial fulfillment of the requirements for the degree of Doctor of Philosophy.

Dominquez, J., and Roesset, J. M. (1978). "Dynamic stiffness of rectangular foundations." *Research Report R78-20*, M.I.T., Cambridge, Mass.

Gazetas, G., Dobry, R., and Tassoulas, J. L. (1985). "Vertical response of arbitrarily-shaped embedded foundations." *J. Geotech. Engrg.*, ASCE, 111(6), 750–777.

Gazetas, G., and Tassoulas, J. L. (1987). "Horizontal damping of arbitrarily shaped embedded foundations." *J. Geotech. Engrg.*, ASCE, 113(5), 458–475.

Hatzikonstantinou, E., et al. (1989). "Rocking stiffness of arbitrarily shaped embedded foundations." *J. Geotech. Engrg.*, ASCE, 115(4), 457–472.

Kausel, E., and Ushijima, R. (1979). "Vertical and torsional stiffness of cylindrical footings." *Research Report R76-6*, M.I.T., Cambridge, Mass.

Kausel, E., and Roesset, J. M. (1975). "Dynamic stiffness of circular foundations." *J. Engrg. Mech.*, ASCE, 101(12), 771–786.

Lysmer, J. (1980). "Foundation vibrations with soil damping." *Civil engineering and nuclear power*. Vol. II, ASCE, New York, N.Y., 1–18.

Roesset, J. M. (1980). "Stiffness and damping coefficients of foundations." *Dynamic response of pile foundations: analytical aspects*, ASCE, New York, N.Y., 1–30.

Tassoulas, J. L. (1986). "Dynamic soil-structure interaction." *Boundary element method in structural engineering*, ASCE, New York, N.Y.

Wolf, J. P. (1985). *Dynamic soil-structure interaction*. Prentice-Hall, Inc., Englewood Cliffs, N.J.

Appendix II. Notation

The following symbols are used in this paper:

A_b = area of basemat;
A_{wr} = area of sidewall that is perpendicular to direction of motion;
A_{wt} = area of sidewall that is parallel to direction of motion;
a_0 = $\omega B/V_s$ = nondimensional frequency;
B = semiwidth of rectangle circumscribed to base surface, as shown in Fig. 1;
C_{br} = contribution to radiation damping from basemat;
C_r = radiation damping coefficients ($r = rx$ or ry);
C_{wr_1} = contribution to radiation damping from rocking sidewall due to its rotation;
C_{wr_2} = contribution to radiation damping from rocking sidewall due to its vertical motion;
C_{wt} = contribution to radiation damping from sidewall in torsion;
c_j = dimensionless damping coefficients ($j = 1,2,3$);
D = trench depth;
d = sidewall height with complete sidewall-backfill contact;
G = shear modulus of soil;
$I_b(I_{bx},I_{by})$ = area-moments of inertia of basemat about x- or y-axis;
I_{wr} = area-moments of inertia of sidewall that is perpendicular due to direction of motion about its axis of rotation;
I_{wt} = polar-moment of inertia of sidewall that is parallel to direction of motion, about axis or rotation, x or y;
L = the semilength of rectangle circumscribed to base surface, as shown in Fig. 1;
V_{La} = $3.4\ V_s/[\pi(1 - \nu)]$ = "Lysmer's analog" velocity;
V_s = velocity of shear waves;
β = frequency-independent material hysteretic damping ratio;
Δ = distance of rocking sidewall from rotation axis;
ν = Poisson's ratio;
ρ = mass soil density; and
ω = circular frequency.